Available online at www.sciencedirect.com

ScienceDirect

Procedia Manufacturing 34 (2019) 738–746

Procedia MANUFACTURING

www.elsevier.com/locate/procedia

47th SME North American Manufacturing Research Conference, Penn State Behrend Erie, Pennsylvania, 2019

Implementation of hybrid additive manufacturing based on extrusion of feedstock and milling

Paolo Parenti*, Salvatore Cataldo, Alberto Grigis, Marco Covelli, Massimiliano Annoni

[a]*Politecnico di Milano, Department of Mechanical Engineering, Via La Masa 1, 20156, Italy*
**Corresponding author. Tel.: +39-02-2399-8530; E-mail address: paolo.parenti@polimi.it*

Abstract

In the current industry, fabrication of metallic and ceramic artifacts by means of feedstock extrusion additive manufacturing is receiving attention because of the capacity of this technology to deal with low costs and materials that possess a low Additive Manufacturability Index when treated with high power beam technologies. However, the extrusion additive manufacturing lacks in achievable accuracy and productivity therefore techniques that can improve the overall performances are required to increase the impact that this technology can have on industry. This paper demonstrates how extrusion additive technology of metals and ceramics can be enhanced by integrating green-state milling into the manufacturing cycle. In the hybrid cycle, the additive and subtractive processes act alternatively on the green-state part to shape its near-net form. This work shows how this innovative method, that integrates cutting and micro-cutting operations on the feedstock, allows compensating the lack of accuracy and micro reachability that characterize the extrusion-based additive manufacturing method. In the manuscript, the promising aspects of the hybrid concept are presented and discussed. Some examples of manufactured parts are illustrated showing how complex geometries, with good surface quality can be addressed with higher production flexibility. The developed hybrid machine prototype adopted for that scope is described along with the AISI316L parts that are obtained by depositing, green-state milling, debinding and sintering the feedstock. Another contribution is provided regarding the feedstock machinability that is studied under different cutting conditions. The feasibility of the hybrid implementation is confirmed and future steps to improve the process are discussed.

Keywords: Hybrid Manufacturing, Additive Manufacturing, feedstock, AISI316, Metal Injection Molding, Shape Deposition Manufacturing, milling, green-state machining

1. Introduction and State of the Art

The development of Additive Manufacturing field enabled the growth of hybrid technologies, which is the proper combination of additive and subtractive manufacturing, installed on the same machine or working together. Many of these techniques consist in the integration of additive directed energy deposition (DED) with subtractive CNC machining within a highly mobile multi-axis machine tool but also in laser-bed fusion (SLS) or wire welding technologies are adopted [1]. Hybrid manufacturing is becoming more popular in industrial applications because of its capability to leverage the advantages of both processes. AM allows to create complex geometries, but with a poor surface quality. Subtractive manufacturing, on the other hand, allows to realize precision components, but with a limited complexity level. As a result, a part with complex geometries and organic designs can be manufactured with the desired surface finish. The common objective that can be pursued by a hybrid approach is a net-shaped part to be obtained in the shortest possible time. Moreover, highly complex parts with external and internal features or high geometrical precision and surface quality can be produced. However, there are disadvantages of this technology that are enclosed in the complexity of process planning and in the cost of the hybrid equipment that sometime could exceed that of the two independent additive and subtractive systems. The fact that the additive and subtractive operations are carried out on the same piece of equipment makes the interference check critical and makes the process planning and operating sequence more complex.

10.1016/j.promfg.2019.06.230

At the same time, industry is putting lots of interests in the last period on binder-based technologies for additive manufacturing of metals and ceramica, such as the extrusion freeform fabrication EFF [2-3], thanks to their capacity of dealing with many materials with cost savings and system simplicity benefits [4-5]. There are systems now ready for the market such as *Desktop Metal Studio System+, Markforged Metal X* that can produce parts exploiting green-shaping deposition through extrusion and parts sintering.

Not only steel, but the extrusion freeform fabrication (EFF) can ideally be adopted with all the materials that are easy to sinter, therefore copper, carbides and ceramics are among the ones that can easily be treated with the EFF and not with the high-power beam technologies [4-6]. EFF allows also the production of multi-material objects. Laser or electron beams additive techniques used to produce near net shape parts through solidification of melted metal powder layers have some disadvantages. First, the implementation of a power beam has higher costs for set-up and maintenance and increased safety problems must be addressed in comparison to EFF. The beam technologies are also more sensible in respect to the powder quality. Dust formation and aging or oxidizing phenomena of the powder must be considered. At the time EFF has some design limitations that mainly relate to the constraints of debinding and sintering processes. Despite debinding and sintering are probably the most challenging aspects of binder-based AM technologies, the shaping deposition process can alter the overall performance and product quality, and therefore needs to be adequately controlled [7]. Tight connection between sintering performances and deposition strategies could exist, therefore the entire process chain must be studied when good results are needed.

One key point of the EFF is that the adopted feedstock material has many similarities with the Metal/Ceramic Injection Molding (MIM/CIM) process and therefore most of the knowledge about debinding and sintering is already available in the proper markets, i.e. MIM/CIM parts manufacturer or more in general, powder metallurgy specialists [5].

Use and development of new binders that can reduce debinding times, increase the sintered parts density as well as the productivity of the overall cycle are in study both in academia and big industrial companies.

Among the many, layer thickness is one of the critical parameters for augmenting the productivity during the deposition process, as in standard FDM (Fused Deposition Modelling) of polymers, but its value is usually constrained by the achievable density and overall surface quality of the parts, which typically decreases when layer thickness increases.

Considering these premises, the process chain involving green-state deposition through EFF could benefit from a hybrid approach where milling process is integrated into the cycle [8].

The adoption of milling in EFF can improve the surface quality (of both external and internal faces), the achievement of thin/small geometrical features and the part dimensional control (considering the shrinkage that the parts undergo during the production cycle). Finally, thanks to the possibility to onboard finish the green parts with milling and to the fact that milling runs much faster than deposition [9-12], higher extrusion deposition rates can be adopted by unaltering the final part quality, thus increasing the overall production rate.

This paper shows the implementation of the hybrid concept that involves extrusion freeform fabrication and milling. The aim is to demonstrate the feasibility of the approach applied to metallic feedstock.

A description of the hybrid machine prototype and the entire process chain is given, followed by an in-depth discussion on the parameters that affect the part quality. Then, green-state milling is discussed along with examples of machined products that are then sintered to generate final parts.

2. Hybrid process chain

The process chain that involves the EFF of ceramic and metals, Fig. 1, starts from the feedstock production or alternatively from commercial MIM/CIM material. The feedstock is then processed by the extrusion machine that deposits the first part layers on the worktable.

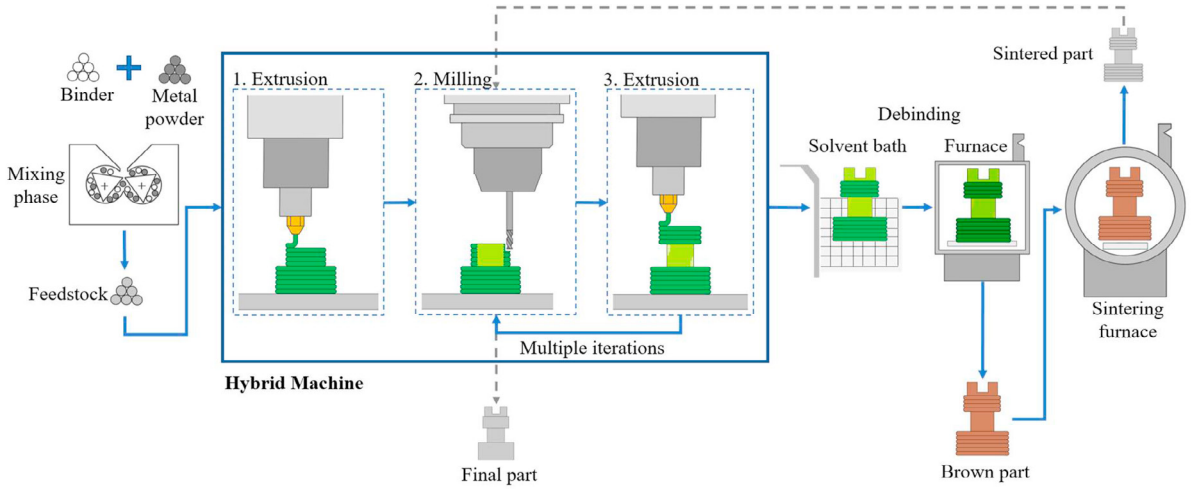

Figure 1: Scheme of hybrid manufacturing involving EFF and milling [8]

After some layers, as soon as enough consistency is generated on the part, milling can enter the process to further shape the geometry and surfaces. The presence on the same machine of two heads for additive and subtractive manufacturing allows easy implementation of alternated depositions and milling passes which can be performed based on the required features and geometrical specifications. This capacity allows the obtaining of internal cavities with tight tolerance specification or more in general, the increase of the productivity for a defined accuracy target. At the same time, milling can be applied in multiple moments of the process chain to improve the accuracy of the green-part and therefore improve the shrinkage compensation (which is done by imposing a controlled part oversizing). Milling can also be applied after the sintering operations to finish functional surfaces, but in this case new working placements are needed.

After the part is shaped, the green body undergoes debinding phases which consist in solvent and/or thermal debinding steps depending on the binder type and the total binder volumetric content. For example, water debinding cycle can be used to remove, when present, the waxes constituents from the binder while thermal cycle is typically needed to remove the thermoplastic resin binder residues. One of the most important steps with some feedstock material is to assure that binder does not leave any carbon residues or other that may alter the final part composition. At the same time, part design must deal with wall thickness limitation to avoid troubles in the debinding phase, whereas an extremely bulk part would require longer debinding times. After debinding, the brown part is characterized by augmented fragility so particular care must be taken in moving the parts. Then, sintering operation allows the part densifying of the component, the closure of voids and microcavities and obtaining the final mechanical properties required. In this last step, it is fundamental to take under control the dimensional variation of the components especially in the presence of bulk workpieces and tiny/slender microfeatures because part distortion may alter the part quality.

Sintered parts must be sufficiently dense and have the required mechanical resistance and it is worth to mention that this latter point is not only affected by the geometry but also by the adopted deposition strategies and achieved surface finishing.

2.1. Extrusion deposition

Extrusion deposition quality depends upon several factors. The driving parameters are illustrated in the fishbone diagram of Fig.2. Stand-off/hatch distance, extrusion velocity, plate and extruder temperatures are those that have the most influence on the deposition quality. Once feedstock and nozzle diameter are selected, experimental investigations can be conducted to find the optimal working windows for those parameters.

There are leading requirements for the extrusion that first consist in avoiding nozzle clogging. Adhesion between subsequent layers must then be guaranteed (each layer must attach to previous ones). No air voids should remain after part sintering and therefore a complete infill must be assured in the feedstock deposition phase. Extrusion parameters must also guarantee a homogenous binder dispersion in the green part.

2.2. Green-state milling

Selection of the most proper cutting tool type and size is required depending on the geometrical feature's dimensions, feedstock composition, heated bed adhesion properties and machine characteristics. Use of coated cutting tools and cooling air can be prescribed to avoid tool clogging due to material adhesion and tool wear, in case of highly abrasive feedstock

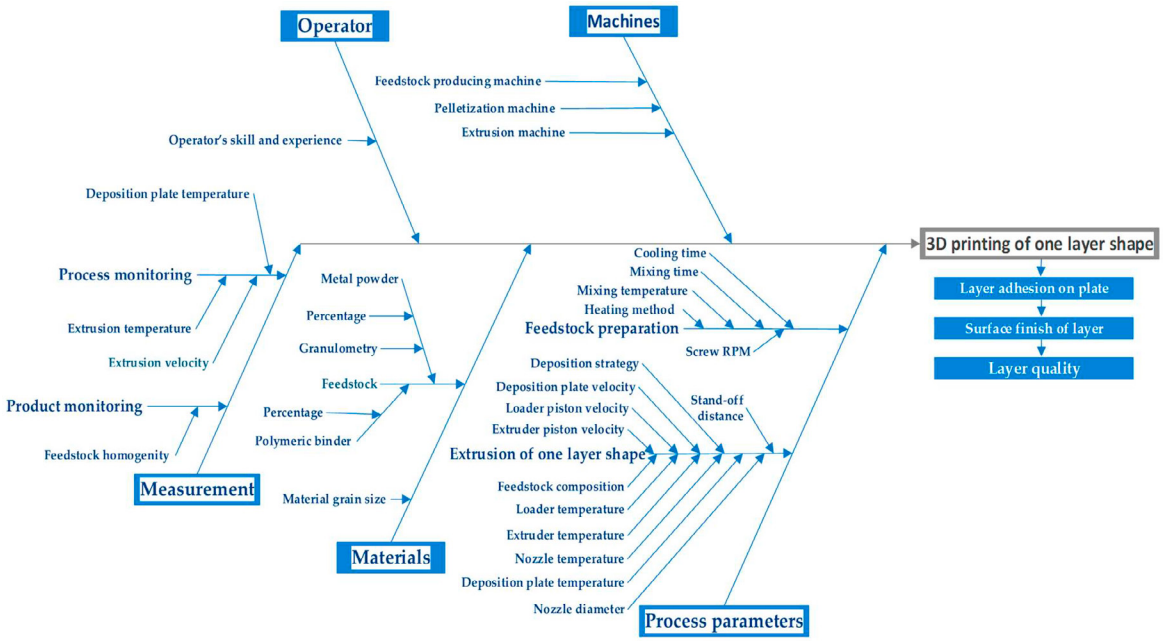

Figure 2: Fishbone diagram of extrusion additive manufacturing of metallic/ceramic feedstock

like ceramic ones. Cutting forces and acceleration rates limit the material removal obtainable in milling since the parts are not adequately anchored to the depositing heated bed. Heated bed material and temperature can be appropriately selected to improve this limit. At the same time, the machine must be capable of performing accurate interpolation trajectories at high speed, especially in the case of smaller tools. Milling can be prescribed for flattening or contouring irregular deposited surfaces or in the presence of critical internal features to finish. In this case, deposition and milling of pure binder component can be used to foster the generation of good internal surface finish. A machine implementation with double extrusion heads is a good solution for that. At the same time, green machining can be adopted with materials that show poor machinability at the sintered state, e.g. ceramic.

Since green parts contain high volumetrically content of binder and do not have particles links, they have lower mechanical properties compared to the brown and sintered parts. Therefore, there are advantages of green-state machining that consist in less forces, less thermal stresses and consequently less tool wear. Precise dimensions can be obtained in terms of part shape together with good finished surfaces (as reported in terms of roughness values in paragraph 4.3). Tools for green machining can be less expensive since induced cutting stresses are lower. By controlling the cutting process, it is also possible to obtain higher density packing after sintering.

In green-state machining, chip removal mechanism differs from the standard metal cutting where the tool induces plastic deformations and slip planes for the chip formation. In green machining different phenomena turns in action as the particle displacements inertia, the viscous behavior of the binder and its thermal softening and in some cases even the particles fracturing [10,13].

The machinability of the green parts depends a lot on the feedstock and binder characteristics. The binder type, its mechanical strength and the quantity inside the powder define the mechanical strength of the feedstock. With these, there are other characteristics that play a role such as part porosity, grain size, toughness, hardness and strength and also elastic and thermal properties. Since these parameters are many, usually experimental approaches are adopted to assess the green machinability index of the material.

It must be considered that green machining can be used only on components that have the necessary mechanical strength to withstand the pressure action produced by the tool during the operation. Clamping of the parts is also an important aspect, especially when additive produced components cannot be glued or fixed before cutting. The cutting process parameters must be set in order to avoid cracks or breakage of the components and keep low values of resultant cutting forces. A proper parameter setting must also consider the obtainable surface quality, since milling of green component can easily lead to surface integrity defects affecting the upper edges and the entrance and exit zones, especially when thin features are machined.

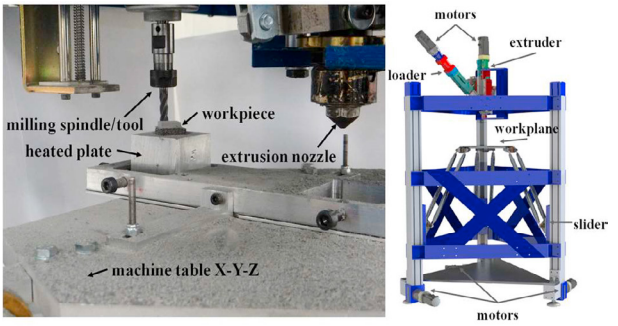

Figure 3: Machine prototype developed in house

3. Materials and Method

3.1. Hybrid prototype

A machine prototype was developed in-house exploiting a two-piston extruder that was designed specifically, starting from an injection molding commercial product, Fig. 3.

A similar concept was developed by Lin et al. used in a novel hybrid additive-manufacturing technique (HASM) with the implementation of a six-DOF axis robot equipped with two types of heads for extrusion and subtractive manufacturing processes [14].

It is possible to feed the loader through a hopper, with feedstock granules that are preheated by the resistors in the plasticizing chamber. Once the input material is heated in the plasticizer (or charger) for a few minutes, it is possible to activate the piston that pushes the material through the plasticization spheres (maximum piston stroke 77 mm) into extrusion chamber. The volume of a full extruder charge is 9000 mm^3 (14 mm in diameter) and it is pushed by the extrusion piston towards the nozzle. Due to its bulkiness, the extrusion head is rigidly connected to the ground while the working plate is handled by a specific handling system.

Regarding the machine architecture, a *Linear Delta* with 3 translational degrees of freedom allows moving the working plane in the x-y plane to deposit a layer and along the z-axis to proceed in height. This reduces the size and complexity of the final machine. It also avoids vibrations that occur during the rapid change of direction due to the high inertia forces that decrease the surface quality of the printed parts. This kind of kinematics is chosen in order to improve rigidity, precision and dynamics. The electric motors are controlled using a PID system through three control loops (current, speed and position). They move three sliders and give the desired movement to the work plane. The maximum working area is 250x250 mm whereas the maximum printing area is 200x200 mm and the maximum printed weight is 8 kg, with maximum available extrusion pressure of 22 MPa [15-16].

To allow the hybridization, a machining spindle that can rotate faster than 10 krpm was installed close to the extruder nozzle. It can move on a vertical slide to retract when not in use and is controlled by a proper driver, commanded by a potentiometer that is connected to the machine PLC and pulpit control. It can fit tools as big as 10 mm in diameter. It is certified to have low runout thus permitting the use of tiny tools

down to less than 0.5 mm, enabling microcutting operations [17].

In the experiments, milling operations were carried out on both the hybrid prototype and an ultra-precise micromilling machine (Kern Evo), with 2-flute carbide flat end milling tools (PVD coated, cutting edge radius of about 8 µm ranging from 0.5 mm to 6 mm in diameter, tested up to 100 m/min of cutting speed and in the range of 30%-100% of axial and radial immersions (i.e. depth of cuts divided by the tool diameters) in flattening and contouring modes. The feed per tooth was set in the range of 5-40 µm. Air chilled at 5 °C was supplied to refrigerate the cutting area and avoid chip accumulation.

3.2. Feedstock preparation

The feedstock adopted in all the experiments was produced in-house and was designed in terms of metal grain dimension, binder type and binder volumetric content. The base material tested consists in a commercial AISI316L powder (D50 = 8.8 µm, density = 7.9 g/cm^3) produced by atomization by *Sandvik Osprey (UK)*. The adopted binder is a commercial water-soluble material produced by eMBe (type *Embemould K83*) with a density = 1.05 g/cm^3. A 60 % volumetric percentage (92 % in weight), was adopted as typical in Metal Injection Molding applications. A twin screws compounder (*Brabender Plasti-Corder*) was adopted for feedstock mixing, Fig.4. Homogeneous feedstock was obtained by optimizing the mixing time and mixing temperature in the range of 30 min and 140 °C respectively. Pellets of ϕ2.5 mm x L10 mm were then produced to feed the extrusion deposition process.

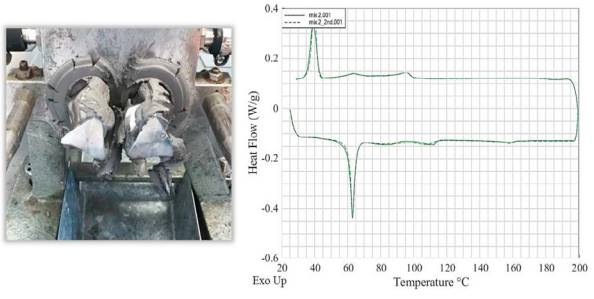

Figure 4: Twin screw mixer used for feedstock preparation and DSC analysis

DSC (Differential Scanning Calorimetry) analysis was used for characterizing the melting points of the solely binder constituents, affected by many factors such as binder composition and not least by the presence of metal particles in the feedstock. The DSC analysis shows that 3 main components with a minimum melting point of about 63 °C and a maximum melting point of about 118 °C are present in the mixture, Fig.4. The extrusion temperature is varied between 90 °C and 140 °C and consists in the temperature of the mixing chamber of the extruder. Nozzle and plasticizing piston temperatures were always set equal to the extrusion temperature.

4. Green shaping processes

4.1. Extrusion deposition strategies and slicing software

According to the process chain, parts must be oversized due to the chip removal operations and the shrinkage occurring during debinding and sintering. Once the CAD drawing is properly scaled, an STL file is produced [1]. Being used for over 30 years with Fused Deposition Modelling printers, the STL file format has become the Rapid Prototyping industry's standard data transmission format.

A critical point is the conversion from STL, obtained by CAD, to ISO G-code file, done by software called slicer.

In this paragraph, the comparison between three different well-known slicers is showed in order to select the best one based on their capacity of coping with metallic feedstock deposition with different geometries and structures.

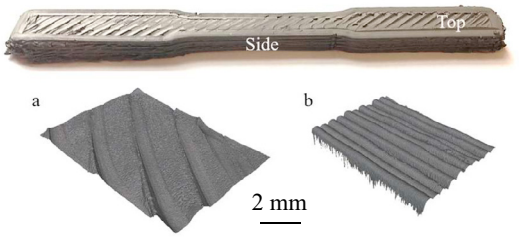

Figure 5: 3D image from *3D microscopy*. (a) top surface; (b) lateral surface

Each software required different slicing parameters to generate the deposition path. It must be considered that the studied software have similar architectures and design but define different deposition parameters and strategies. Since the software require different setup and types of parameters for running a cycle, the comparison is performed by considering the best parameter set for each one.

Usually, parts are sliced in horizontal layers to generate plane movements in x-y directions.

The different features and parameters that are required are the *shells perimeters* that define the surface quality, the *infill* which represent the internal pattern used to fill up the part, the *skirt/brim* that are aimed at fostering the adhesion with the plate, the *hatch distance* which represents the distance between

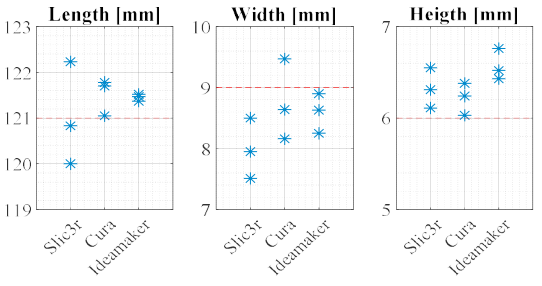

Figure 6: Real specimens dimensions compared to the nominal ones (red dashed lines).

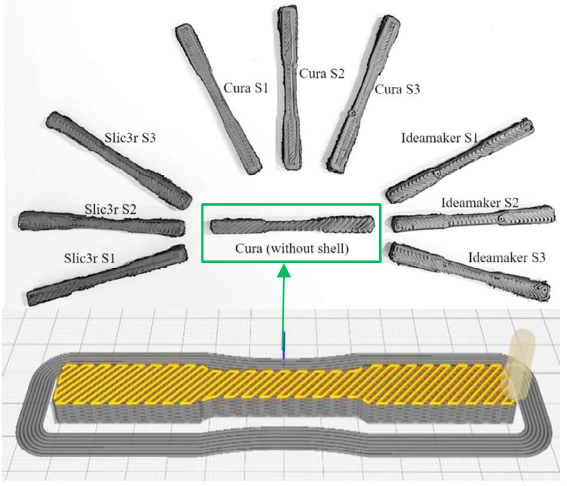

Figure 7: Slicing trajectory (without shell/perimeter) and specimens produced with 3 different slicers

Table 1: Ranking of the achievable quality with the three slicers basing on three functions: absolute appearance, lateral surface quality, top surface quality (I: *Ideamaker*, C: *Cura*, S: *Slic3r).*

Absolute	Lateral surface	Top surface
I2	*I1*	*C1*
C3	*I2*	*C3*
C1	*C3*	*C2*
C2	*C1*	*I2*
I3	*C2*	*I3*
I1	*I3*	*I1*
S2	*S3*	*S1*
S3	*S1*	*S2*
S1	*S2*	*S3*

two deposited wires and the *layer height* which indicates the vertical distance between each deposited layer.

In addition, printing parameters must be set in order to obtain the desired components. Feedstock temperature is controlled by heating resistors inside the extrusion head. Heated bed ensures a proper attachment of the first deposited layer. Plane movement speed and nozzle diameter should be a trade-off between productivity, material adhesion and part accuracy.

To test the influence of the slicer characteristics, a comparison was run by empirically testing the three slicers to obtain the best samples they could produce for a defined geometry.

Each slicer has an optimal field in which the component shows the best characteristics, so the best choice would be to use different slicers for different products and features. The choice was guided by the main open-source software used in FDM production. *Cura*, *Slic3r* and *Ideamaker* were the three software selected for the comparison.

The methodology consisted in the following step. Starting from dog-bone STL specimens (whereas the dog-bone shape was designed according to the Standard ASTM E8/E8M), G-codes were created with the slicers. Three samples were

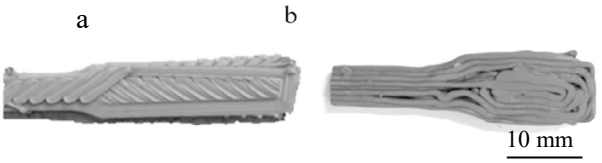

Figure 8: Deposition strategy. (a) zig-zag 45°; (b) concentric.

obtained with each software (with nominal dimension: length = 121 mm, height = 6 mm and

width = 9 mm) by empirically optimizing the deposition. Quantitative comparison analysis was conducted on top and lateral surface roughness and dimension, Fig.5-6, using 3D microscopy (*Alicona G4)*.

Moreover, qualitative analyses were conducted by observing the visual aspect, the consistency and visible defects of the samples, Fig.7, Table 1. Deviation from nominal dimension was mainly due to different amount of extruded material and perimeter losses. Nine specimens were tested and coded*, Fig.7*.

Ideamaker revealed to be the best option to obtain a good external quality of components. *Cura* was the most complete and flexible software; it was possible to choose many different options that can affect the final component and can help the final user in building complex and difficult 3D structures. *Slic3r* showed many criticalities in the specimen production giving high sensitivity to shell/perimeters breakage and voids generation. All the slicers showed a tendency to generate wider and taller feedstock workpieces, Fig. 6, due to the plowed areas on the specimen's surfaces. No systematic bias, however, was observed in length of the specimens but large dimension dispersion was observed among the replications for all the software. This variation, that could be associated with the extrusion process variations in relation to feedstock characteristics, remained constant for all the three software indicating a minor role of the slicing strategy.

With slender pieces, where a dimension is predominant to another, cooling rate can be quicker than the deposition rate, therefore limiting the inter-adhesion property of the layers and eventually causing layer cracking. Maximum distance between adjacent points was found to be related with the deposition rate and the feedstock material used. Basing on this observation, the most suitable infill method was found.

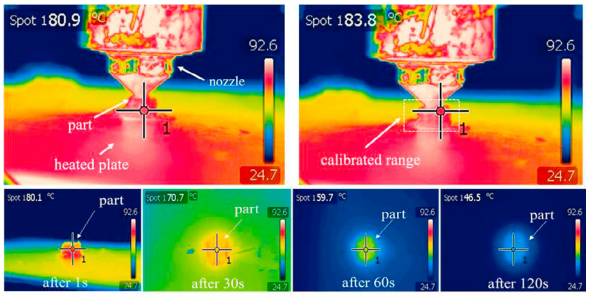

Figure 9: Infrared images taken during extrusion of cube samples 20x20x10 mm (taken with Flir T-Series thermal Imaging System)

Under slender workpiece conditions, a 45°(zig-zag) infill is preferable to the standard 90° (concentric) method (Fig. 8). For shapes close to circular form the two methodologies did not reveal so much difference. Though, the 45° infill configuration was selected because it could also provide an improvement of the machinability of the parts, as explained in paragraph 4.2.

In a second extend, the extrusion temperature management was found to be critical. The heated bed and extrusion temperatures must be appropriately adjusted to have enough fluidity to be able to print complex geometries. Then, the deposition strategy must consider also some temperature related variables as part geometry and component heat capacity. The heated bed temperature was tuned by trial and error testing with starting conditions that were selected based on DSC analysis of the feedstock. Extrusion temperature played also a role on the optimal bed temperature values. In the tested cases, the adopted heated bed temperature was ranging from 70-80 °C.

The use of an infrared camera was suitable in the carried out tests for supporting the above setup of the temperature values. Extrusion monitoring could be a viable way to keep under control and understand the deposition of new layers upon the already deposited ones that are colder. Indeed, thermal imaging (Fig. 9) provides useful information detecting possible cold spots and so probable cracks in those areas. In case the two previous options revealed not to be enough, ad hoc deposition strategies could be implemented by the slicing software and infrared lamps could be properly activated to provide the required heat. The preliminary testing of this monitoring technique confirms that in-process monitoring can be implemented but specific design of the measurement system must be provided.

Moreover, thermal imaging could help in reducing the overheating during milling process by allowing the adaptation of cutting parameters to avoid binder segregation that could be detrimental for the final part mechanical properties.

4.2. Deposition strategy selection for improving part machinability

In general, milling must be adopted when specific finished features are required, like slots with sharp edges, flat surfaces, precise holes or complex free-form geometries with low scallop heights. Since milling is much faster than extrusion, it could be adopted to compensate rougher (but faster) depositions, producing an overall increase of productivity and accuracy.

However, process planning of extrusion and milling must be done conjunctly by considering the two processes since there is interaction between them.

Nowadays, there are commercial software, like Siemens NX, that are specifically designed for hybrid cycles involving additive and subtractive manufacturing, but they mainly address laser beam additive technologies, with limited flexibility to address feedstock extrusion processes. On the other side, when dealing with FDM slicers as the tested ones, typically adopted with polymers deposition, the needs and constraints of a hybrid implementation involving milling are not taken into consideration. For this reason, specific adjustments were required and were developed in this work.

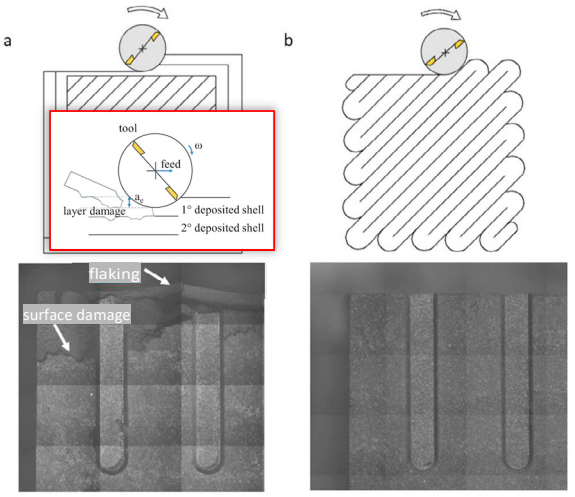

Figure 10: Shell/perimeter milling (a), Infill milling (b)

All the dog-bone specimens deposited with the three different software, discussed in paragraph 4.1, were milled in green-state on their external surfaces, in order to understand which printing solution could better support the parts machinability.

A second geometry was studied during the experimental printing campaign consisting in simple cubic samples with the main purpose to study the layer integrity before and after milling and to test the cutting of micro slotting on the sample top surface (Fig. 10). The slots geometry was selected also for analyzing the cutting forces and the achievable roughness on the milled components.

It was found that milling tool and the induced cutting forces tended to damage the parts and the deposited green-part strands. Two main situations occurred. The first consists in the damages of the upper part surface during flattening (Fig. 11 (f)) operation. In this case, a single layer detachment was usually observed, mainly concentrated at the part outer borders, leading to localized, but shallow, defects typically bigger than the adopted milling tool diameter.

The other case is represented by the damages happening when contouring the part. In this case, cracking formation and shell detachment were systematically observed when the shell/perimeter deposition strategy was adopted. Large extension of the defects typically happened thus limiting the capacity to obtain good parts. The reason could be linked to localized lack of adhesion between the outer shells with the inner one that, under cutting forces, produced a complete fracture of the shell. This phenomenon was exacerbated by the adoption of large radial amount of depth of cuts (a_e in Fig.10 (a)). To avoid this defect, a deposition strategy without shell/perimeters was selected. Infill was deposited with an orientation of 45° and phase-shifted by 90° between each layer, Fig.10 (b).

4.3. Green-part machinability

The feedstock material machinability depends upon many factors. Multiple testing was executed on the produced feedstock both in terms of milling and micromilling operations.

Tests of green parts executed with a sensorized machining center confirm that milling forces keep low when machining AISI316L green feedstock [17]. The cutting pressure resulted in the order of 1/10 of the bulk material. Workpieces could then sustain the forces and did not detach from the bed during the cutting operations.

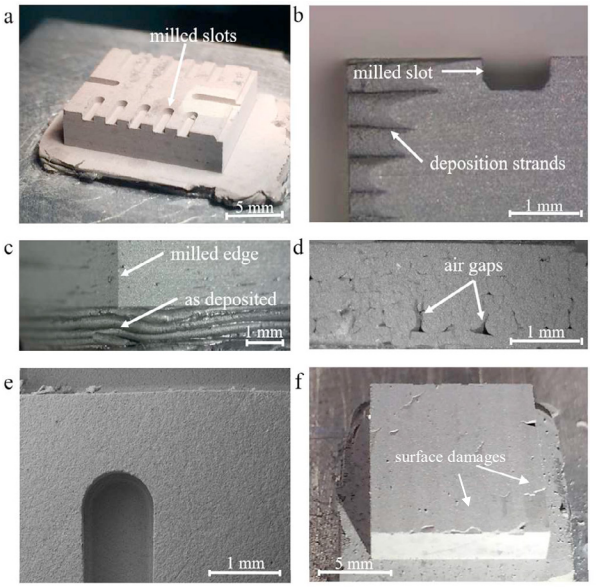

Figure 11: Micromilled parts at green-state (a), (b), edge quality on green part (c), air gaps on green part (d), milled slot on brown part (e), surface defects in green-part (f)

Chip clogging and chip entrapment in the cutting area was observed during cutting when cooling air was not provided. Air cooling then resulted capable of refrigerating and cleaning the contact area improving the machining results. Despite the use of cooling air, workpiece bulk temperature seemed to play an effect on the achievable surface quality. This is an important aspect for the process planning since after deposition, the cooling rate of the samples is quite slow, as can be observed in Fig. 9. Since hot milling could be prescribed to reduce the overall cycle time, feedstock must possess high machinability also in hot-state.

Surface appearance of the green-state milled samples was good and homogeneous without any apparent defects nor relevant milling marks.

Milling operations were able to remove all the surface irregularities. The overall surface roughness of the deposited workpiece, originally around Sa ~ 70-120 µm, was reduced to Sa = 1.4-2.8 µm in the top and lateral green part surfaces.

Some upper border damages appeared in the green part because of air-gap formations (Fig. 11 (d)). Without taking these local defects into consideration, an average Sa of 2.5 µm was achieved on the sintered workpiece.

Good sharp edges were obtained with a radius lower than 100 µm, Fig. 11 (c). The Scanning Electron Microscopy (SEM) conducted on milled feedstock revealed the achievement of no surface voids with extremely sharp corners (Fig. 11 (b) and (e)). Little binder segregation was observed in some cases, Fig. 12 (a), often aligned with the deposited strands direction. However, this did not generate noticeable problems in the sintered workpieces.

4.4. Debinding and Sintering

The type of debinding action for removing the binder from the green part strictly depends upon the type and quantity of binder adopted. In the tested case, a water debinding followed by thermal debinding were adopted for all the samples.

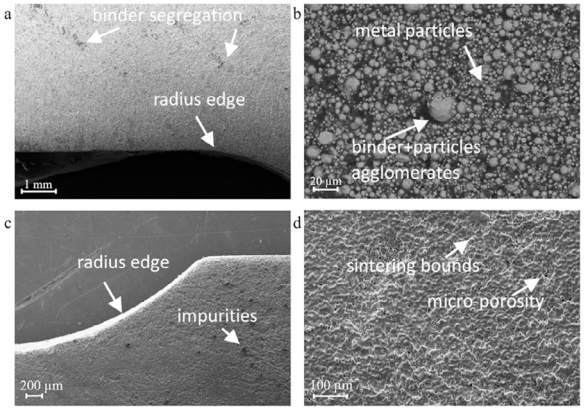

Figure 12: SEM analysis of green milled parts (a), (b), and of sintered parts (c), (d)

Water soluble binder was adopted and therefore a stirring equipment with recirculating water at a temperature of 50 °C was adopted for 10 hours. Samples were weighted showing residual percentage of binder around 2.5-4% in weight, likely related to the backbone binder content in the mix, removable only by a thermal cycle.

Thermal debinding and pre-sintering phases were conducted in hydrogen furnace at 680 °C for 10 hours. The brown and pre-sintered components showed enough resistance and an overall good integrity with no visible damages to features and surfaces, Fig. 11 (e). No cracks were observed, however negligible binder residues appeared in the SEM analysis of the upper surface of the brown parts.

Then subsequent sintering was done in a 3% argon tube furnace at a temperature of 1340 °C (1 hour), following the prescription of the feedstock manufacturer.

A linear shrinkage of about 11.5 % occurred after sintering. The components looked unaltered except for some small pores due to deposition inaccuracies affecting some samples nearby the upper corners and microcavities visible in the SEM analysis Fig. 12 (d). Despite this fact, an overall density of 88-92% was

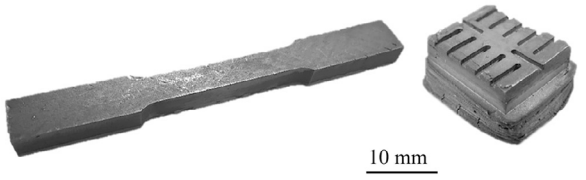

Figure 13: Some produced AISI316L parts after sintering

achieved on those sample without any apparent internal delamination or cracking, as shown in Fig.13.

The produced samples are now undergoing mechanical characterization to assess the material functional performances.

5. Conclusion

Among the several influencing facotrs that affect the tested AISI316L feedstock extrusion deposition process, the most important aspects resulted, above all, the extrusion temperature and the deposition strategy. Interlayer adhesion and perimeter generation played a key role for the generation of air gaps free samples.

Milling of green-state feedstock resulted a viable way to improved surface finish and obtain fine features with accurate dimension on the green parts, that could resist to debinding and sintering stages. Deposition strategies were designed to support the machinability by avoiding layer detachment due to cutting forces.

Machinability of the soft AISI 316L resulted good, comparable with hot pressed material, with low achieved forces that vary non-linearly with feed rate and show only slight changes by varying the workpiece base temperature.

The given examples promote this novel hybrid manufacturing approach, based on additive extrusion and machining of feedstock, as a future tangible solution for the industrial production of metallic and ceramic artifacts.

Future attention will be given to the mechanical characterization of the produced components, to the design of a novel machine architecture and to the testing of innovative materials for the AM field [18].

Acknowledgements

The authors are grateful to V. Mussi (Musp) and G. De Gaudenzi (Films S.p.A.) for their support.

References

[1] Flynn J. Hybrid Additive and Subtractive Machine Tools-Research and Industrial Developments Hybrid Additive and Subtractive Machine Tools- Research and Industrial Developments. Int J Mach Tools Manuf 2015;101:1–45. doi:10.1016/j.ijmachtools.2015.11.007.

[2] Kruth JP, Leu MC, Nakagawa T. Progress in additive manufacturing and rapid prototyping. Ann CIRP 1998;47:525–40.

[3] Greulich M. Rapid prototyping of functional metallic parts. Comput Ind 1995;28:23–8.

[4] Ampower insights, Additive manufacturing sinter based, https://am-power.de/en/insights/additive-manufacturing-sinter-based-technologies/

[5] Gutierrez JG, Cano S, Schuschnigg S, KuklaC, Sapkota J, Holzer C. Additive Manufacturing of Metallic and Ceramic Components by the Material Extrusion of Highly-Filled Polymers: A Review and Future Perspectives, Materials 2018;11: 840.

[6] Deckers J, Vleugels J, Kruth JP. Additive manufacturing of ceramics: A review. J Ceram Sci Technol 2014;5:245–60. doi:10.4416/JCST2014-00032.

[7] Cristofolini I, Rao A, Menapace C, Molinari A. Journal of Materials Processing Technology Influence of sintering temperature on the shrinkage and geometrical characteristics of steel parts produced by powder metallurgy. J Mater Process Tech 2010;210:1716–25. doi:10.1016/j.jmatprotec.2010.06.002.

[8] Parenti P, Cataldo S, Annoni M, Shape deposition manufacturing of 316L parts via feedstock extrusion and green-state milling, Manufacturing Letters, 2018; 18: 6-11.

[9] Salak A, Selecka M, Danninger H, Machinability of powder metallurgy steel, First Edition, CISP- Cambridge International Science Pubblishing, Cambridge UK, ISBN 1-898326-82-7.

[10] Dadhich P, Srivas PK, Mohanty S, Dhara S. Microfabrication of green ceramics: Contact vs. non-contact machining. J Eur Ceram Soc 2015;35:3909–16. doi:10.1016/j.jeurceramsoc.2015.06.025.

[11] Ghazanfari et al, A novel extrusion based additive manufacturing process for ceramic parts, Solid Freeform Fabrication Symposium, January 2016

[12] Du W et al, A Novel Method for Additive/Subtractive Hybrid Manufacturing of Metallic Parts, 2016, 1018:1030.

[13] Li J et al, Micromachining of pre-sintered ceramic green body, Journal of Materials Processing Technology, 2012; 571-579.

[14] Li, Lin, Azadeh Haghighi, and Yiran Yang. A novel 6-axis hybrid additive-subtractive manufacturing process: Design and case studies, Journal of Manufacturing Processes, 2018; 33:150-160.

[15] Rane K, Cataldo S, Parenti P, Sbaglia L, Mussi V, Annoni M, Giberti H, Strano M, Rapid production of hollow SS316 profiles by extrusion based additive manufacturing. AIP Conference Proceedings 2018; 1960, 140014, https://doi.org/10.1063/1.5035006

[16] Annoni M, Giberti H, Strano M. Feasibility Study of an Extrusion-based Direct Metal Additive Manufacturing Technique. Procedia Manuf 2016;5:916–27. doi:10.1016/j.promfg.2016.08.079.

[17] Kuriakose S, Parenti P, Cataldo S, Annoni M, Micromilling of metallic feedstock produced by extrusion additive manufacturing, Proceedings of World Congress of Micro and Nano Manufacturing (WCMNM2018), September 2018, Slovenia.

[18] Bourell D, Kruth JP, Leu M, Levy G, Rosen D, Beese AM, et al. Materials for additive manufacturing. CIRP Ann - Manuf Technol 2017;66:659–81. doi:10.1016/j.cirp.2017.05.009.